IEEE Access
Multidisciplinary | Rapid Review | Open Access Journal

Digital Object Identifier 10.1109/ACCESS.2022.DOI

Improving Indoor Localization Using Mobile UWB Sensor and Deep Neural Networks

LEYLA NOSRATI[1], MOHAMMAD SADEGH FAZEL[1], AND MOHAMMAD GHAVAMI[2], (Senior Member, IEEE)

[1]Department of Electrical and Computer Engineering, Isfahan University of Technology, Isfahan 84156-83111, Iran
[2]Electrical and Electronic Engineering Department, London South Bank University, London SE1 0AA, U.K.

Corresponding author: Leyla Nosrati (e-mail: l.nosrati@alumni.iut.ac.ir).

ABSTRACT Accurate localization in indoor environments with ultra-wideband (UWB) technology has long attracted much attention. However, due to the presence of multipath components or non-line of sight (NLOS) propagation of the radio signals, it has been converted to a critical challenge. Existing solutions use many fixed anchors in the indoor environment. Particularly, large areas require many anchor points and in the case of unexpected events that lead to the destruction of existing infrastructures, the fixed anchor points cannot be used. In this paper, a novel localization framework based on the transmitting signal from a mobile UWB sensor on the outside of the building and its received signal regarding the modified Saleh Valenzuela (SV) channel model is presented. After preprocessing the received signals, two new procedures to reduce the ranging error caused by multipath components are proposed. In the first procedure, two machine learning algorithms including multi-layer perceptron (MLP) and support vector machine (SVM) using the extracted features from the received UWB signal time and power vectors are implemented. Moreover, in the second procedure, two deep learning algorithms including MLP and convolutional neural networks (CNNs) using the received UWB signal time and power vectors are implemented to improve the performance of the indoor localization system. The simulation results show that the architecture designed for the convolutional neural network based on the hybrid dataset (the combination of the dataset related to received UWB signal time and power vectors) provides a mean absolute error (MAE) of about 3 cm.

INDEX TERMS UWB, Multipath components, Indoor localization, Machine learning, Mobile sensor.

I. INTRODUCTION

INDOOR localization has attracted much attention since people spend most of their time inside buildings. Some critical applications and services based on indoor localization such as emergency rescue, fire brigade, or incident management need an easy-deployable localization system that can provide high accuracy localization in indoor environments. There are two effective methods to localize the target. In the first method, it is assumed that the target's position is calculated using the navigation sensors and then provided to a monitoring station. In the second method, the target does not have these sensors, its position at the monitoring station is calculated by transmitting radio signals. The problem of localization becomes complicated when the operations need to be carried out in a closed environment such as indoors. Global navigation satellite systems (GNSS) are the most widely used localization technology for outdoor applications. In indoor environments, however, their signals can be easily blocked, attenuated, or reflected. Localization through preinstalled radio infrastructures (e.g. Wi-Fi access points, RFID or Bluetooth tags) have been applied in indoor environments, but there is no guarantee that all of them have these radio infrastructures and even if they do, may not be suitable for accurate localization. The alternative approach is based on UWB technology. The benefits of UWB technology include high data rate, high time resolution, high bandwidth, low-cost equipment, and power spectral density (PSD) level much lower than Wi-Fi and Bluetooth, which makes it suitable for indoor applications [1]–[4]. Although the UWB technology has high time resolution versus multipath, in most cases, because of existing multipath components and NLOS conditions, the signals containing the target information, are comparable to noise levels and may be buried among the strong multipath components. As a result, the need for complex

algorithms and new approaches to detect the accurate special target information is doubled. Most investigations have been conducted on indoor localization using a UWB radar which is installed inside of the building, or is static on the walls on the outside of the building. However, it requires an expensive infrastructure of many fixed anchor points (nodes with known positions that can be used as a transceiver). Also, the number of necessary anchor points increases by growing the size of the area where UWB devices are deployed [5], [6] and the fixed anchor points cannot be used in the case of unexpected events that lead to the destruction of existing infrastructures.

In this paper, a novel method to resolve these issues is suggested. Since mobile sensors have high flexibility and mobility, they can be used as aerial anchor points with no limitation on the number of them and the areas that they can be flown. Also, they can be easily used in the case of unexpected events. Hence, we use a mobile UWB sensor and the proposed procedures to improve indoor localization accuracy.

II. RELATED WORK

In previous similar investigations, authors often use Wi-Fi, ZigBee, and Bluetooth technologies for indoor localization [7]–[12]. In [7] the authors combined the received signal strength indicator (RSSI) fingerprint and kernel-SVM learning approach for indoor localization based on Wi-Fi technology. In this paper, by using the hybrid kernel instead of the single kernel and increasing the size of the training set, indoor localization performance was improved. Their simulation results disclosed that by using the proposed algorithm, the position estimation error is equal to 1.81 meters. The authors in [8] proposed a principal component analysis-based support vector machine (PCA-SVM) approach by using the received signal strength (RSS) signals for indoor localization based on Wi-Fi technology. Their results showed, the PCA-SVM method provides a mean localization error of 1.37 meters, which is a significant improvement compared to K-nearest neighbor (KNN) and SVM methods, which have mean localization errors of 3.08 and 1.76 meters, respectively. In [9] by using the RSS and channel state information (CSI), the authors presented a deep learning approach for indoor localization based on Wi-Fi signals. The indoor localization was considered as a classification problem. Their simulation results showed that by using CSI information and CNN algorithm, a maximum localization error of 0.92 meter with a probability of 99.97% was achieved. In [10] by using a series of the RSSI measurements, the authors proposed recurrent neural networks (RNN) algorithms for indoor localization based on Wi-Fi fingerprinting. Their simulation results showed that by using the proposed long short-term memory (LSTM) structure, an average localization error of 0.75 meter can be achieved. In [11] an affordable indoor localization system based on Bluetooth low energy (BLE) technology was proposed to monitor the location of a target that carries a BLE beacon. The location of the target inside the building by using the RSSI and trilateration and fingerprinting based methods was estimated. Their simulation result showed that by the fingerprinting-based method, a localization accuracy above 90% was achieved. In [12], the design and implementation of a wearable device for localization of Alzheimer's patients, based on the RSSI and ZigBee technology were presented. To improve the localization accuracy, a back propagation-based artificial neural network (BP-ANN) algorithm was used. Their simulation result showed that the mean localization error in the testing phase was 0.921 meter.

The basic problem of using the above technologies is the need for long-term measurements and sophisticated calibration procedures. On the other hand, according to the results provided in the related works, these technologies cannot obtain a precision of a few centimeters for indoor localization. It is noteworthy in most cases (such as unexpected accidents and natural disasters), a localization system is needed to estimate a target's position with an accuracy of a few centimeters in the shortest possible time. The UWB technology attracted great attention in indoor localization problem because of its precision of a few centimeters, very high bandwidth, wall penetration, high time resolution [13] and [14]. However, the practical expansion of this technology has many challenges, including multi-user interference, multipath effects and NLOS propagation [15]–[18].

In the literature, authors use the multipath channel statistics such as kurtosis, mean excess delay (MED), root mean square (RMS) of delay spread, signal amplitude, and CSI to identify the NLOS conditions or mitigate the ranging error by machine learning algorithms including Gaussian process (GP), SVM and MLP [19]–[21]. In [22] without feature extraction and based on raw channel impulse response (CIR) data and CNN algorithm, authors have shown that NLOS conditions can be detected and consequently, the ranging error has reduced. Results in [22] showed that the performance of the indoor localization system is improved by using the predicted NLOS conditions and ranging error information, in combination with least squares (LS) and weighted least squares (WLS) location estimation algorithms. Authors in [23] proposed a feature-based localization approach by using a deep long short-term memory (DLSTM) algorithm for UWB localization. Their results showed that by using the extracted features from the user's distance information and the DLSTM algorithm, the mean localization error of 0.05 meter can be achieved. The authors in [24] proposed a deep gated recurrent unit (DGRU) algorithm by using the time series data generated from the UWB channel. Their simulation result showed that the proposed GRU-based localization method can achieve a root mean square error (RMSE) of 0.8 meters compared to their proposed CNN-based localization method. In [25] a neural network structure based on a deep auto encoder-back propagation (DAE-BP) algorithm by using time difference of arrival (TDOA) value of UWB received signal have been proposed to provide high accuracy in indoor localization problem. The simulation results showed that the DAE-BP can reach mean square error (MSE) of 0.03 meter.

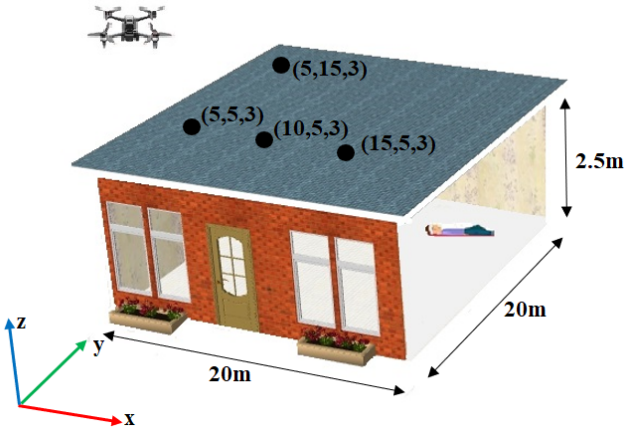

FIGURE 1: In the proposed system, the mobile UWB sensor flies to four known positions. At each position, the received signals are preprocessed and then used to estimate the target position.

III. MAIN RESULT AND ORGANIZATION

The main contributions of this paper are as follows:

- In the previous works, fixed UWB anchor points have been used to localize people indoors. However, in this paper, it is proposed to perform indoor localization more effectively and efficiently by a mobile UWB sensor outside a building.
- We consider direct and indirect rays reflected from the target and the received signal is influenced by multipath components. It is not necessary to have the line of sight link in the channel model. Unlike the papers [19]–[22] that use machine learning algorithms to identify NLOS conditions or mitigate the ranging error, in our paper, to alleviate the ranging error and estimation of target's position, two procedures are proposed. In the first procedure, some features are extracted from the received UWB signal time and power vectors and used as the input for each of the two machine learning algorithms including MLP and SVM. In the second procedure, the target's position is estimated based on the received UWB signal time and power vectors using MLP and CNN algorithms (without feature extraction).
- By using simulation results we show that if both time and power measurements of the received UWB signal from the modified SV channel are used as input to the CNN algorithm, a significant improvement in the performance of the indoor localization system can be achieved.

The rest of this paper is organized as follows: Section IV describes the system model and data collection based on the modified SV channel model. In section V, the proposed procedures are discussed in detail. In section VI, the numerical analysis of two suggested procedures is evaluated. Also, validation of the second procedure with two related works is performed. Finally, section VII is the conclusion of this paper.

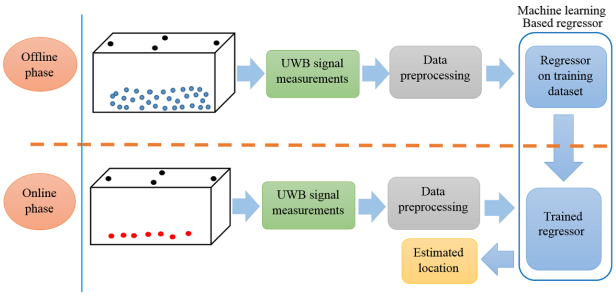

FIGURE 2: Flowchart for achieving the indoor localization by machine learning based algorithms.

IV. SYSTEM MODEL

The desired model for indoor localization using a mobile UWB sensor is presented in Fig. 1. In this figure, the mobile UWB sensor (for example a small size quadrotor) as an aerial anchor with height of 3 meters flies to four different known positions outside of a building with dimensions of $20 \times 20 \times 2.5\ m^3$ to to find the 2D position of a target that is placed on the floor inside the building. It should be noted that at least three anchor points are necessary for this kind of localization. Using more anchor points, the accuracy of the localization algorithms is increased, but on the other hand, the computational complexity, flight time, and energy consumption of the mobile sensor are also increased, which are not desirable. Here, to achieve an appropriate accuracy with low computational complexity, we have considered four anchor points in our system model. Because the UWB technology is used for short-range indoor applications due to low emission levels allowed [26], we assumed that the round trip distance of the mobile UWB sensor from the target is less than 20 meters. In this paper, the indoor localization problem is formulated using machine learning algorithms, such as SVM, MLP, and CNN, which can be solved in two phases: off-line training and online localization phases. A flowchart that includes both off-line training and online localization phases is presented in Fig. 2. According to this figure, in the off-line training phase, the target is placed randomly at many different known positions (small blue points). For each of these positions, the mobile UWB sensor sends and receives the signal at four known anchor points (black points). After preprocessing of the data, the regressor (SVM, MLP, and CNN) which describe the relationship between UWB signal measurements and the corresponding target positions is learned with the achieved training dataset. In the online localization phase, the target is placed randomly at some different unknown positions (red points). For each of these positions, the mobile UWB sensor sends and receives a UWB signal at four known anchor points (black points). After preprocessing of testing data, the target location is estimated by using the trained regressor.

A. DATA COLLECTION

Since, as in [22], access to the laboratory environment is not always possible, to create the raw synthetic dataset, it is necessary to provide a suitable channel model. In the following, the modified SV channel model based on the IEEE 802.15.4a channel model [27], is represented.

The impulse response of the modified SV channel model is described as follows [28]:

$$h(t) = \sum_{l=0}^{L} \sum_{k=0}^{K} \beta_{k,l} e^{j\theta_{k,l}} \delta(t - T_l - \tau_{k,l}) \tag{1}$$

where, L, K, T_l, $\tau_{k,l}$, $\beta_{k,l}$, and $\theta_{k,l}$ are the number of clusters in the channel, the number of multipath components within each cluster, the arrival time of the first path of the l^{th} cluster, and the arrival time, amplitude and phase shift of k^{th} path within the l^{th} cluster, respectively. Also, $\delta(.)$ is the Dirac delta function. The leader power of l^{th} cluster $(\beta_{0,l})^2$ and the arrival time of the first path of the l^{th} cluster (T_l) calculated as follows [29]:

$$20\log_{10}\beta_{(0,l)} = p_t^{dBm} + 10\log_{10}\left(\frac{c^2}{(4\pi d f_c)^2}\frac{1}{(1-(\frac{w}{2f_c})^2)}\right) \tag{2}$$

and

$$T_l = \frac{2\left\|x_{val} - x_t\right\|_2}{c} \tag{3}$$

where p_t, c, and d are the transmitter power, the speed of light, and the distance between the transceiver and the related virtual node, respectively. Also, w and f_c indicate the bandwidth and central frequency, respectively. Moreover, x_t and x_{val} are the position of the transceiver and virtual node respectively. Also, $\|.\|_2$ is the Euclidean norm operator. According to [27] we assume that the arrival time of k^{th} path within the l^{th} cluster $(\tau_{k,l})$ is modeled by combining two Poisson processes with signal reception rates λ_1 and λ_2 as follows:

$$\begin{aligned}\Pr(\tau_{k,l}|\tau_{(k-1),l}) = \alpha\lambda_1 \exp\left[-\lambda_1(\tau_l - \tau_{(k-1),l})\right] + \\ (1-\alpha)\lambda_2 \exp\left[-\lambda_2(\tau_l - \tau_{(k-1),l})\right]\end{aligned} \tag{4}$$

In this respect, α is the probability combination factor. The average power of the k^{th} path within the l^{th} cluster $(\beta_{k,l})^2$ decreases linearly with time constant of γ from its own leader power. Moreover, Nakagami distribution is used to model the small-scale fading part of $\beta_{k,l}$. In Nakagami distribution, the shape parameter m is modeled as log-normally distributed random variable whose logarithm has a mean of σ_m and standard deviation of μ_m. The channel phase shift is uniformly distributed between $[0, 2\pi]$. It should be noted as we consider only the amplitude of the received signal in our approach, we do not need to consider the phase shift of the channel component.

Fig. 3 shows an example of the outline of the modified SV channel model. As shown in this figure, each cluster has some multipath components and the signal power decreases as time passes. Considering all of these information increase the complexity of localization algorithms. In this paper, it is suggested to use the received raw UWB signals from the modified SV channel up to the second cluster leader as inputs to the localization algorithms to decrease the computational complexity and have fewer multipath components in localization algorithms input. The received UWB signal time and power vectors in each cluster are calculated according to algorithm 1.

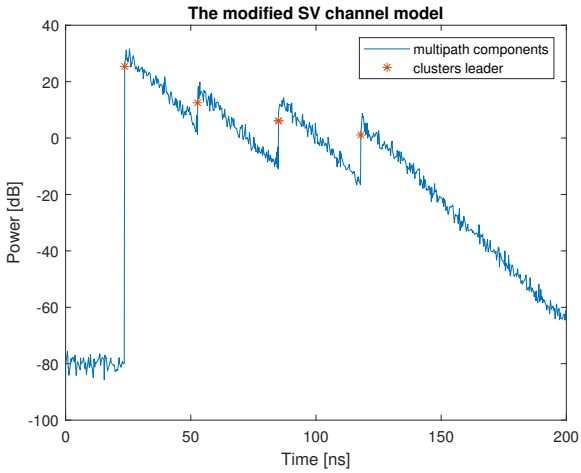

FIGURE 3: An example of the outline of the modified SV channel model. The red asterisks are the clusters leader and each cluster has some multipath components.

Algorithm 1 Calculate the received UWB signal time and power vectors

Input: p_t, c, d, w, f_c, x_t, x_{val}
Output: The received UWB signal time and power vectors
Calculate $\beta_{0,l}$ based on Equation (2)
Calculate T_l based on Equation (3)
Calculate $\boldsymbol{RAY}$ as the matrix to save the received signal time and power of paths in each cluster as follows:
$\boldsymbol{RAY}(\mathbf{0},\mathbf{1}) = T_l$
$\boldsymbol{RAY}(\mathbf{0},\mathbf{2}) = \beta_{0,l}$
$k = 0$
while $\boldsymbol{RAY}(\boldsymbol{k},\mathbf{1}) < T_{l+1}$ **do**
$k = k + 1$
$\boldsymbol{RAY}(\boldsymbol{k},\mathbf{1}) = \tau_{k,l}$
$\boldsymbol{RAY}(\boldsymbol{k},\mathbf{2}) = 20\log_{10}\beta_{(0,l)} - \frac{\boldsymbol{RAY}(\boldsymbol{k},\mathbf{1})}{\gamma} + \zeta$
end while

V. PROPOSED METHODS

Machine learning algorithms have gained a lot of attention in recent years. The reason is that, they do not need complex mathematical equations and achieve low energy consumption and cost. Therefore, in this paper, two procedures based on machine learning algorithms are presented to estimate the target's position indoors. In the first procedure, the location-dependent useful information is extracted from the received UWB signal time and power vectors and used as input for

each of two machine learning algorithms including MLP and SVM. In the second procedure, without feature extraction, the received UWB signal time and power vectors are used as inputs for two deep neural networks, including MLP and CNN. In this section, the two proposed procedures, as well as the designed architecture in each of them are described in detail.

A. FIRST PROCEDURE

In this procedure, for the SVM and MLP algorithms, the target is placed at N and M different random positions, respectively. For each of these positions, the mobile UWB sensor sends and receives the UWB signal at four known anchor positions. For each algorithm, 60%, 20%, and 20% of measurements for N or M target positions are selected randomly for training, validation, and testing samples, respectively. The validation samples are used to watch the training procedure and prevent the network from overfitting. Overfitting refers to the gap between the training loss and the validation loss, which increases as the training loss decreases after some training epochs. Regarding four anchor points, each training sample contains a 28-feature vector including the time delay of the first and second cluster leader, received average power, maximum received power, the number of multipaths, mean excess delay (MED) and kurtosis [20]. These features are extracted from the received UWB signal time and power vectors. Also, to compare the performance of the SVM and MLP algorithms, we use the mean absolute error (MAE) criterion defined as follows:

$$\mathrm{MAE} = \frac{\sum_{i=1}^{p} |s'_i - s_i|}{p}. \tag{5}$$

where, p is the number of test samples, s and s' denote the actual and predicted target position, respectively.

1) Regression with SVM

SVM is a supervised learning method that applies to both classification and regression problems. In this paper, indoor localization is considered as a regression problem. The objective is to establish a functional dependence between the feature vectors and the specific target position (the Cartesian coordinate of the target) based on the training samples and then to determine the position of the target test samples according to their characteristics. Assume that a mobile UWB sensor flies to four known positions with coordinates (x_i, y_i), $i \in (1, 2, 3, 4)$ as transceiver outside of the building. In the training phase, the target is randomly assigned to N' positions with coordinates $r_n = (\acute{x}_n, \acute{y}_n)$, $n \in (1, 2, \ldots, N')$. The column vector of the extracted features from the received UWB signal time and power vectors is $\boldsymbol{c_n} = [\boldsymbol{v_{1,n}}, \boldsymbol{v_{2,n}}, \ldots, \boldsymbol{v_{4,n}}]^T$, where $\boldsymbol{v_{i,n}}$ represents the feature vector with dimensions 1×28 for the i^{th} anchor at the n^{th} position of the target. Therefore the training set can be written as $(\boldsymbol{c_n}, r_n)$ $n \in (1, 2, ..., N')$. On the other hand, since the extracted features do not have the same range of values, the learning operation may take a long time. Hence, in order to have high accuracy and faster convergence, before the model learning, the target positions and feature vector are normalized separately such that all normalized values will be between zero and one. Using the normalized samples, the regression function for SVM learning model is expressed as follows [20]:

$$f(\boldsymbol{c_n}) = \langle \boldsymbol{w}, \psi(\boldsymbol{c_n}) \rangle + b \tag{6}$$

where, $\boldsymbol{w} \in R^4$ is the weight parameter vector and the inner product operator is performed by $\langle , \rangle$. Moreover, $b \in R$ shows the bias in the network. Due to the complexity of the signal propagation within an environment, the relationship between the feature vector and the locations is nonlinear, thus $\psi(.)$ is a nonlinear mapping function that maps the feature vector from low dimension space to high dimension space. To obtain optimal values of the weight parameter vector ($\boldsymbol{w}$) in (6), the author [7] proposes solving the following optimization problem:

$$\underset{\boldsymbol{w},\xi,\eta}{\text{minimize}} \ \frac{1}{2}\|\boldsymbol{w}\|_2^2 + C\sum_{i=1}^{N'}(\xi_i + \eta_i) \tag{7}$$
$$s \cdot t \cdot \begin{cases} r_i - \langle \boldsymbol{w}, \psi(\boldsymbol{c_n}) \rangle - b \le \varepsilon + \xi_i \\ b + \langle \boldsymbol{w}, \psi(\boldsymbol{c_n}) \rangle - r_i \le \varepsilon + \eta_i \\ \xi_i \ge 0 \ , \ \eta_i \ge 0 \end{cases}$$

where ε and C are the deviation between the regression function and the real position of r_i, and the cost parameter, respectively. Also, ξ_i, η_i are slack variables. The dual formulation of the above SVM problem provides an alternative to solve equation (7). Thus, kernel function approaches can be used to map the data into higher-dimensional spaces. Under the optimal conditions, the equation (6) is expressed as follows [20]:

$$f(\boldsymbol{c_n}) = \sum_{j=1}^{N'} \alpha_j \varphi(\boldsymbol{c_n}, \boldsymbol{c_j}) + b^* \tag{8}$$

where $\varphi(\boldsymbol{c_n}, \boldsymbol{c_j})$ denotes the kernel function. The values of α_j and b^* can be obtained by using the advanced convex optimization facility such as the MATLAB LIBSVM toolbox [31].

2) Regression with MLP

MLP is a class of feedforward deep or artificial neural networks. MLP network consists of three layers: input, hidden and output. In this network, the stochastic gradient descent (SGD) algorithm is used as the training algorithm [32]. The basis of this method is to define a loss function between the predicted and real location. Using the backpropagation (BP) scheme [33], the error of each layer propagates from output to input. Therefore all of the network parameters (weights and biases) are updated iteratively. Generally, as the number of hidden layers in the neural network increases, it becomes more flexible to learn nonlinear relationships, but sometimes it can cause some problems such as overfitting. Hence, in our

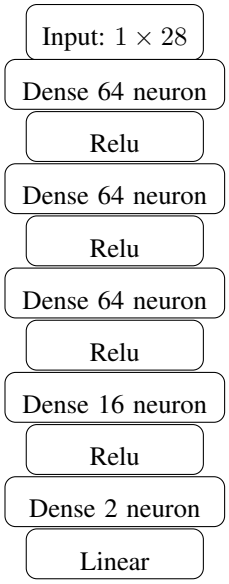

FIGURE 4: The architecture used for MLP algorithm in the first procedure

specific scenario, we need to find the right number of neurons in fully connected (FC) or dense layer in MLP networks by trial and error which does not lead to overfitting. Fig. 4 shows the designed architecture for this type of neural network, which consists of four hidden layers with 64, 64, 64, and 16 neurons per dense layer, respectively. Since the purpose of this paper is 2D target localization, the number of neurons in the output layer is chosen as 2. Using the sigmoid function ($f(x) = \frac{1}{1+e^{-x}}$) in the hidden layers may lead to the vanishing gradient problem. To avoid this problem, a rectified linear unit (ReLu) function ($f(x) = \max(0, x)$) is used as the activation function in each hidden layer [34]. Also, the linear activation function ($f(x) = x$) is not used in the hidden layers, because the composition behind them will still be equivalent to another linear unit and will not improve the network structure. On the other hand, because the output of the network is the continuous values of the target position, the sigmoid or linear continuous activation function can be used in the output layer. Moreover, we use adaptive moment estimation (Adam) to update the parameters of the network [35] because it needs relatively low memory and works well even with the little tuning of hyperparameters and has fast and reliable learning convergence versus SGD. To avoid overfitting problem, the L_2 regularization [36] is adopted.

B. SECOND PROCEDURE

In this procedure, for the MLP and CNN algorithms, the target is placed at M different random positions. For each of these positions, the mobile UWB sensor sends and receives the UWB signal at four anchor positions. For each algorithm, 60%, 20%, and 20% of measurements for M target positions are selected randomly for training, validation, and testing samples, respectively. Here, six different cases can be considered regarding three different datasets (the received UWB signal time and power vectors each with dimensions 1×544, which are calculated according to Algorithm 1, and also their concatenation (hybrid data) with dimensions 1×1088) and two deep neural networks; MLP and CNN. Three different criteria including MAE, the number of training parameters, and the estimation time of each test data are used to compare the performance of MLP and CNN algorithms. The second and third criteria show the degree of network complexity. The more complex the network, the higher computational load. Of course, the lower computational load of the proposed method, the lower need for expensive resources or CPU. Also, the Hyper-parameters such as learning rate, batch size, and the number of epochs, which are set before training, for both of the MLP and CNN algorithms are presented in Table 1.

TABLE 1: The Hyper-parameter of MLP and CNN in the second procedure

Hyper-parameter	Value
Learning rate	0.001
Batch size	32
Epochs	100

TABLE 2: The number of neurons used in MLP algorithm in the second procedure

Dataset	Number of neurons
Received UWB signal time	32,32,32,32,16,2
Received UWB signal power	128,128,64,64,64,64,16,2
Hybrid data	256,256,256,2

1) Regression with MLP

Similar to the previous section, the Relu and linear functions are used as the activation function in the hidden and output layers, respectively. Table 2 shows the best trial and error results we obtained as the appropriate number of neurons in each dataset which do not lead to overfitting. Because the localization problem is in 2D coordinates, the number of neurons in the last layer is chosen as 2.

2) Regression with CNN

In general, CNN consists of input, hidden and output layers. The hidden layer of a CNN typically consists of a series of sublayers such as convolution layers, pooling layers and FC layers [37]. The convolution layers contain several filters. Each of these filters can extract a specific property in different locations of the input data. The pooling layers are used to reduce the number of parameters. Spatial pooling also called subsampling or downsampling, reduces the dimensionality

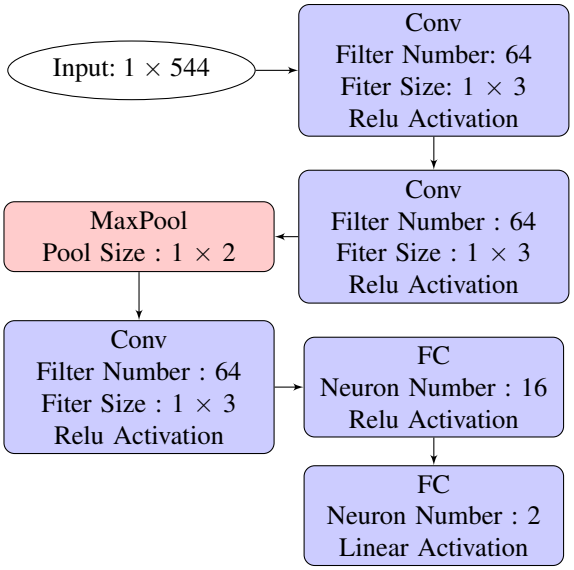

FIGURE 5: The designed architecture to the received UWB signal time dataset in CNN algorithm

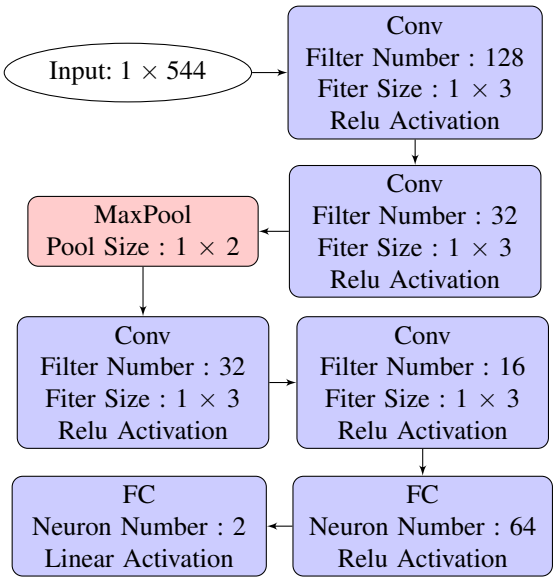

FIGURE 6: The designed architecture to the received UWB signal power dataset in CNN algorithm

of data while retaining important information. After convolution and pooling layers, all data are flattened into a vector and then are fed into FC layers like neural networks. Similar to the MLP network, the Relu function is used in the hidden layers to avoid vanishing gradient problem and the linear activation function is used to perform regression in the output layer. The learning process is similar to the MLP as mentioned in subsection regression with MLP of the first procedure section. In both networks, necessary actions including; 1) using more training data, 2) reducing the network's capacity by removing layers or reducing the number of elements in the hidden layers, and 3) applying L_2 regularization are performed to control overfitting. The appropriate number and size of the filters in convolution layers «Conv», the size of pooling in the pooling layer «MaxPool» and the number of neurons in each dense layer «FC» which do not lead to overfitting, are shown in Fig. 5, Fig. 6 and Fig. 7 for three different datasets.

VI. NUMERICAL ANALYSIS

To create synthetic datasets, at first, the target is placed at 1000, 60,000, and 60,000 different random positions, then for each position of the target, according to Algorithm 1, the received UWB signal time and power vectors are calculated and are used as input to the SVM, MLP, and CNN algorithms, respectively for indoor localization. In this section, the numerical results of these algorithms in both procedures are evaluated. Also to prove the validity and efficiency of the used datasets, we investigate the indoor localization problem based on the proposed approaches in [9], [22], [24].

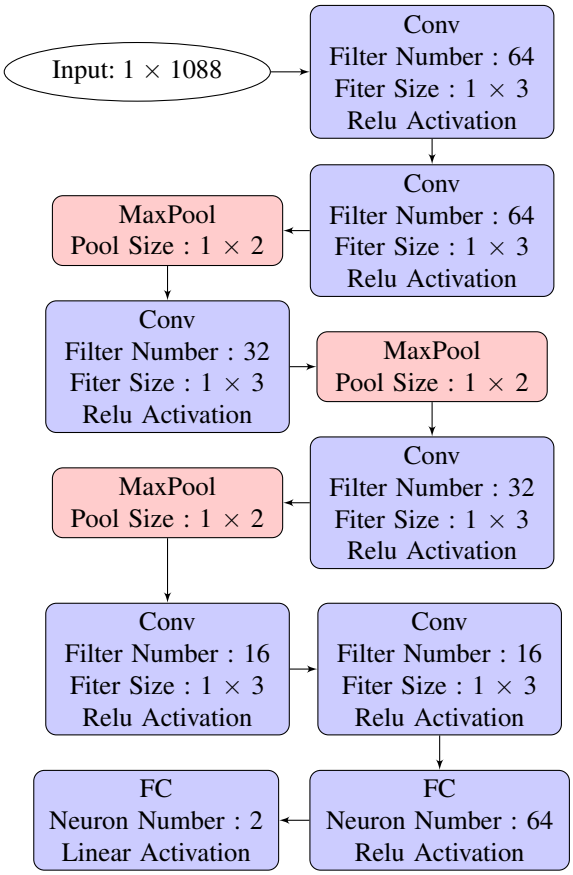

FIGURE 7: The designed architecture to hybrid dataset in CNN algorithm

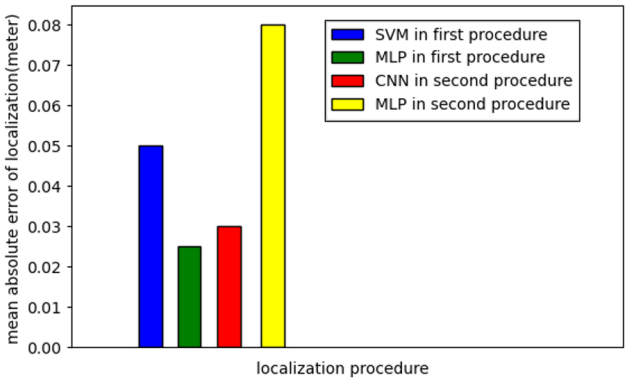

FIGURE 8: Mean absolute error criterion in the SVM, MLP, and CNN algorithms in both procedures

A. COMPARISON OF MLP AND SVM IN THE FIRST PROCEDURE

As mentioned in the previous section, the extracted features from the received UWB signal time and power vectors are provided as inputs to the MLP and SVM algorithms. To compare the performance of these algorithms, the MAE criterion according to (5) is used. The MLP with one hidden layer similar to SVM can only learn small spaces of data. To learn more complex distributed data, we need to increase the number of hidden layers of the MLP. Consequently, as can be seen in Fig. 8, the MLP algorithm in the first procedure provides less MAE than the SVM algorithm in both dimensions of 2D Cartesian coordination.

B. EVALUATION OF MLP IN THE SECOND PROCEDURE

Table 3, shows the result of three criteria for the MLP algorithm in the second procedure. Since the used neural network has no significant complexity, the number of training parameters and estimation time of each test data have an acceptable value for the employed architecture. Therefore, we only use the MAE criterion to evaluate the MLP network for three datasets. Because the UWB signals have high time resolution, according to MAE criteria, the received UWB signal time measurements are more accurate than the received UWB signal power measurements. On the other hand, since the hybrid dataset uses the whole information of both received UWB signal time and power measurements, it provides the lowest MAE.

C. EVALUATION OF CNN IN THE SECOND PROCEDURE

In Table 4, the required time for estimating test data is a very small fraction of the time and the number of network parameters shows an acceptable value for the used architecture. As a result, again the MAE criterion is used to compare the performance of these three datasets. Similar to the MLP algorithm results, the hybrid data set, gives the lowest MAE.

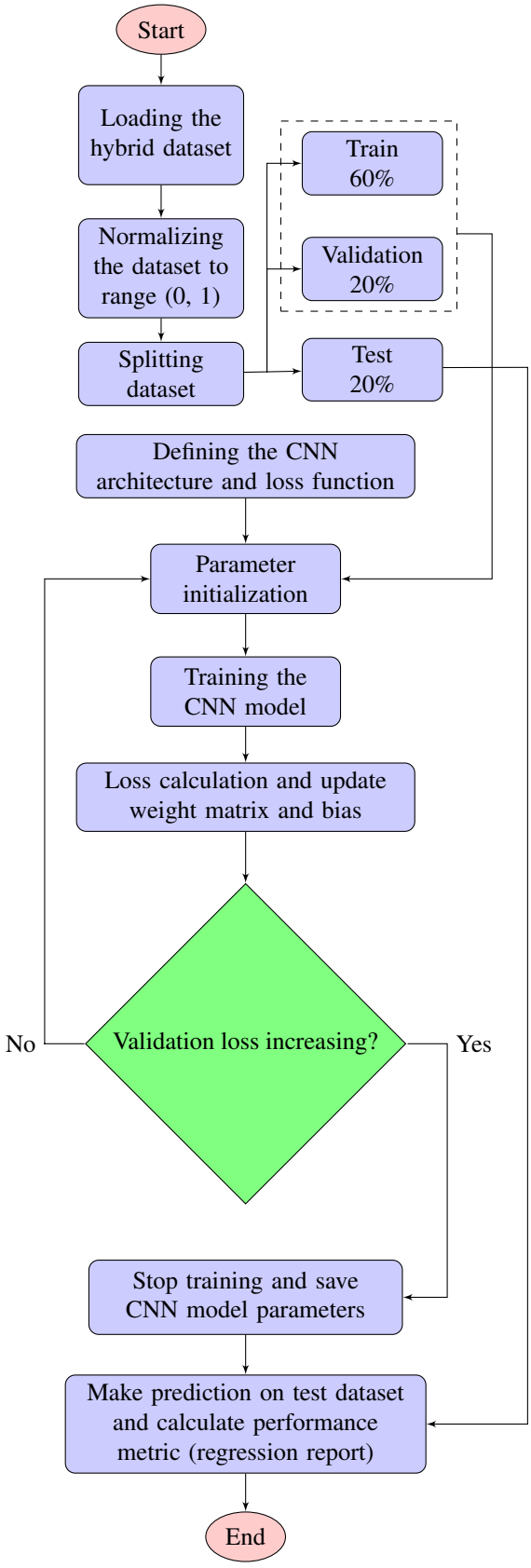

FIGURE 9: Flowchart of CNN algorithm for indoor localization

TABLE 3: Evaluation of the MLP algorithm in the second procedure

Datasets	MAE [m]	Number parameters	Estimation time [μs]
Received UWB signal time	0.09	21170	14
Received UWB signal power	0.20	108082	17
Hybrid data	0.08	408834	32

TABLE 4: Evaluation of the CNN algorithm in the second procedure

Datasets	MAE [m]	Number parameters	Estimation time [μs]
Received UWB signal time	0.04	299442	490
Received UWB signal power	0.08	290066	570
Hybrid data	0.03	156514	1000

D. COMPARISON OF MLP AND CNN IN THE SECOND PROCEDUE

In the MLP algorithm, all input samples are received as a vector and mapped to the feature extraction space, while in the CNN algorithm, the input data vectors are converted to a square matrix then the algorithm filters are locally focused on data sub-matrix and features of each local sub-matrix are extracted individually. By considering the MAE criterion for comparing the performance of these neural networks, as in the Fig. 8, it can be seen that the CNN algorithm shows better performance than the MLP algorithm in the second procedure with the accuracy of 3 cm in each of two dimensions. Moreover, in Fig. 9 the flowchart of the CNN algorithm that has the best result for the hybrid dataset are presented.

E. VALIDATION OF THE SECOND PROCEDURE WITH THREE RELATED WORKS

To prove the efficiency of the used dataset in the second procedure, as in [9], we consider the indoor localization problem as a classification problem. Thus, the 60,000 random locations of the target inside the cube-shaped environment are converted into 16 classes and used as outputs to MLP and CNN networks. Similar to the used architecture in [9] but with little change and trial and error, the best results can be seen in Table 5. However, even if we are more accurate in predicting the target position, because of the large size of the cube-shaped environment, the area of each block is large and after classifying the center of each block as the target location, we will achieve a large quantization error. On the other hand, if we reduce the area of the blocks we would have to increase the number of blocks, so in the final layer of the classification model, we would need a large number of neurons, which in addition to the difficulty in training would so increase the computational burden. To analyze the localization performance we assume that the localization error is equal to the distance between the actual position and the estimated position. Assuming that the estimated position is equal to the center of the estimated block, the highest and lowest value of the MAE for hybrid data with the prediction accuracy of 97.98% and 100% is equal to 62 cm in both cases for x-coordinates, 247 and 245 cm for y-coordinates, respectively. Based on these results, we conclude that the proposed classification without regression method in [9] is not suitable for the used dataset in this paper and leads to a large ranging error.

TABLE 5: Performance summary of various classification methods

Classification method	Number parameters	prediction Accuracy (%)	MAE [m]
MLP_Received UWB signal power	321232	87.68	1.53
MLP_Hybrid data	458448	95.7	1.53
CNN_Received UWB signal power	85600	91.16	1.53
CNN_Hybrid data	303904	97.98	1.53
MLP_RSS [9]	1782576	80.29	0.92
MLP_CSI [9]	1912176	99.93	0.92
CNN_RSS [9]	48288	82.32	0.92
CNN_CSI [9]	132928	99.98	0.92

To test the performance of the proposed localization error reduction method in [22], a dataset with a measured range between the mobile UWB sensor and target should be constructed. Due to lack of access to the DWM1000 IR-UWB module, the measured range (d') and actual distance (d) between mobile UWB sensor and the target is computed as follows:

$$\mathrm{d}' = \frac{c * t'}{2} \tag{9}$$

$$\mathrm{d} = \frac{c * t}{2} \tag{10}$$

where c, t', and t are the speed of light, the time length of

TABLE 6: Accuracy of localization methods for the received signal power dataset

Localization method	MAE in this work [m]	MAE in [22] [m]
LS	4.16	1.05
LS_REG	0.31	0.35
WLS	3.58	0.68
WLS_REG	0.29	0.30

TABLE 7: Accuracy of localization methods for the hybrid dataset

Localization method	MAE in this work [m]
LS_REG_HYBRID	0.10
WLS_REG_HYBRID	0.09

the first cluster, and the arrival time of the first cluster leader, respectively. The best localization performance is achieved when all of the used ranges in the position estimation are within the LOS range. However, due to the presence of multipath components, the measured ranges become positive bias and the position estimation with these measurements in LS and WLS estimators results in a MAE of several meters. These results are presented in the LS and WLS rows in Table 6. According to [22], the ranging error is defined as the difference between the measured range and actual distance ($\epsilon = \mathrm{d}' - \mathrm{d}$) and is used as outputs for training the CNN-based regression model. Also, instead of using the CIR measurements, the received UWB signal power, and hybrid datasets are used as CNN network inputs. By calculating the estimated ranging error and measured range, the estimated distance ($\hat{\mathrm{d}} = \mathrm{d}' - \hat{\epsilon}$) can be obtained. A significant improvement in indoor localization is achieved if the estimated distance is used in the LS and WLS estimators. These results are shown in the LS_REG and WLS_REG rows (two regression method based on LS and WLS algorithms) in Table 6. However, as observed in the previous sections, since the hybrid dataset uses all of the information, therefore according to Table 7 it shows a lower MAE when the estimated distance is used in the LS and WLS estimators.

To prove the efficiency and high accuracy of the used sequential dataset (time and power vectors of the received UWB signal) in the second procedure, as in [24] we consider the indoor localization problem as a regression problem. The architecture of the proposed GRU-LE model in [24] is illustrated in Fig. 10. According to this figure, the model consists of one input layer, two GRU layers, three fully connected layers, and one regression layer. The output of the model is the estimated 2D location of the target. The input data, which is generated from the received UWB signal

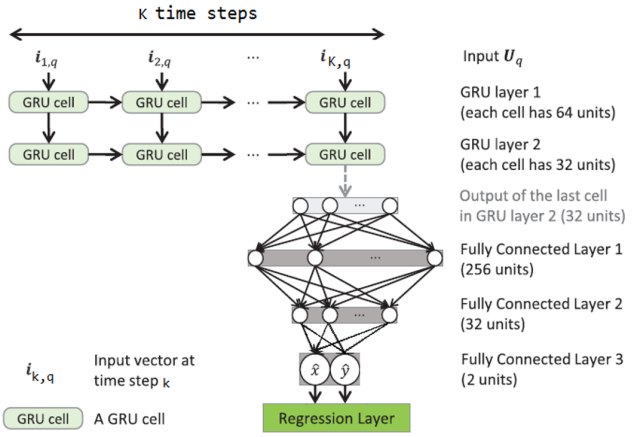

FIGURE 10: The GRU-LE model architecture [24]: The input is generated from algorithm 1, and the output is the 2D position of the target.

time or power, is a matrix $\boldsymbol{U}_q \in \mathbb{R}^{I\times K}$, $q \in (1, 2, \ldots, Q)$, where $I \in (1, 2, 3, 4)$ represents the number of known positions of the mobile UWB sensor, and K represents the number of time steps for each q training sample. Also, to generate Q samples for the GRU-LE model, the target is placed in Q different random positions. According to [24], the input matrix of GRU-LE model can be considered as $\boldsymbol{U}_q = [\boldsymbol{i}_{1,q}, \boldsymbol{i}_{2,q}, \ldots, \boldsymbol{i}_{K,q}]$, where $\boldsymbol{i}_{k,q} \in \mathbb{R}^{I\times 1}$ denotes the input vector at k^th time step as shown in in Fig. 10. As it is shown, the number of GRU cells in each GRU layer are same and equal to the number of time steps in the input matrix. The number of units for each cell in the first and second GRU layers and similarly, the number of units for the first two fully connected layers is selected according to [24]. To estimate the 2D position of the target, in the last fully connected layer, two units are used. Finally in the regression layer of the model, the mean square error between the predicted and real position of the target is used as the loss function. To evaluate the performance of the used sequential datasets based on GRU-LE model in indoor localization problem, the RMSE criterion is used as an evaluation metric, which is calculated as follows:

$$\mathrm{RMSE} = \sqrt{\frac{\sum_{i=1}^{p}(s_i' - s_i)^2}{p}} \tag{11}$$

Table 8, shows the result of RMSE criterion for both sequential datasets in the proposed GRU-LE model in [24]. According to this table, a significant improvements compared to [24] in the localization problem are observed by using both sequential datasets.

Finally, the localization error of the proposed methods and previous related works are summarized in Table 9. The second and third columns of the table show the types of wireless technologies and machine learning-based techniques that are used in indoor localization for each research paper. As it is clear, localization methods based on Wi-Fi, Bluetooth, and ZigBee technologies cannot obtain a precision of a

TABLE 8: Evaluation of the sequential datasets in the GRL-LE model

Sequential Dataset	RMSE [m]
Received UWB signal time	0.1
Received UWB signal power	0.2
Received UWB signal in [24]	0.8

few centimeters for indoor localization. On the other hand, the MLP localization technique with extracted features and the CNN localization technique with hybrid data show a significant improvement in indoor localization. It should be noted that by using both sequential datasets, better results in indoor localization problem are observed compared to [24], but our proposed approach nevertheless shows a significant improvement over GRU-LE model in [24]. On the other hand, by using hybrid dataset for training the proposed regression model in [22], an acceptable accuracy in the indoor localization problem is obtained using CNN combined with the WLS localization technique. But due to the structural differences in the used hybrid dataset and quantization error in CNN-CSI localization technique, the proposed approach in [9] does not provide higher accuracy in predicting the target position within each class and therefore the target position cannot be estimated with an accuracy of a few centimeters.

VII. CONCLUSION

In this paper, to reduce the installation cost of the expensive anchor points in the large areas for indoor localization, the use of a mobile UWB sensor, due to having high mobility and low-cost features is presented. Moreover, two procedures for reducing the indoor localization error are proposed using SVM, MLP, CNN algorithms applied on the received UWB signal time and power vectors. In the first procedure, the main features were extracted from the received UWB signal time and power vectors up to the second cluster leader (to have fewer multipath components) and are used as inputs in MLP and SVM algorithms. The simulation results show that the MLP algorithm provides lower MAE than the SVM algorithm because the MLP algorithm uses more hidden layers. In the second procedure, three different datasets were extracted from the received UWB signal time and power vectors up to the second cluster leader and are used as inputs in the MLP and CNN algorithms. Because the CNN algorithm could extract meaningful information from the datasets, it shows lower MAE than the MLP algorithm for the hybrid dataset. Also by comparing the proposed approach with the procedures in the literature, the accuracy and efficiency of the used dataset in the second procedure are proved. In this paper, we used synthetic dataset for investigating the indoor localization problem. In the near future, by providing real dataset achieved by using the mobile UWB sensor, we will show the validity and high efficiency of our proposed procedures in real environment.

ACKNOWLEDGMENT

This article is extracted from the thesis approved and defended in the Faculty of Electrical and Computer Engineering of the Isfahan University of Technology. We would like to express our sincere gratitude to Dr. Nader Karimi, Associate Professor at Isfahan University of Technology for providing us with his laboratory facilities.

REFERENCES

[1] O. Onalaja, M. Adjrad, and M. Ghavami, "Ultra-wideband-based multilateration technique for indoor localisation," IET Communications, vol. 8, no. 10, pp. 1800-1809, 2014.
[2] R. Ye, S. Redfield, and H. Liu, "High-precision indoor UWB localization: Technical challenges and method," in 2010 IEEE International Conference on Ultra-Wideband, 2010, vol. 2: IEEE, pp. 1-4.
[3] S. Monica and G. Ferrari, "Accurate indoor localization with UWB wireless sensor networks," in 2014 IEEE 23rd International WETICE Conference, 2014: IEEE, pp. 287-289.
[4] A. De Angelis, S. Dwivedi, and P. Händel, "Characterization of a flexible UWB sensor for indoor localization," IEEE Transactions on Instrumentation and Measurement, vol. 62, no. 5, pp. 905-913, 2013.
[5] S. Capkun and J.-P. Hubaux, "Secure positioning in wireless networks," IEEE Journal on Selected Areas in Communications, vol. 24, no. 2, pp. 221-232, 2006.
[6] P. Perazzo, L. Taponecco, A. A. D'amico, and G. Dini, "Secure positioning in wireless sensor networks through enlargement miscontrol detection," ACM Transactions on Sensor Networks (TOSN), vol. 12, no. 4, pp. 1-32, 2016.
[7] J. Yan, L. Zhao, J. Tang, Y. Chen, R. Chen, and L. Chen, "Hybrid kernel based machine learning using received signal strength measurements for indoor localization," IEEE Transactions on Vehicular Technology, vol. 67, no. 3, pp. 2824-2829, 2017.
[8] L. Zhang, Y. Li, Y. Gu, and W. Yang, "An efficient machine learning approach for indoor localization," China Communications, vol. 14, no. 11, pp. 141150, 2017.
[9] C.-H. Hsieh, J.-Y. Chen, and B.-H. Nien, "Deep learning-based indoor localization using received signal strength and channel state information," IEEE access, vol. 7, pp. 33256-33267, 2019.
[10] M. T. Hoang, B. Yuen, X. Dong, T. Lu, R. Westendorp, and K. Reddy, "Recurrent neural networks for accurate RSSI indoor localization," IEEE Internet of Things Journal, vol. 6, no. 6, pp. 10639-10651, 2019.
[11] L. Bai, F. Ciravegna, R. Bond, and M. Mulvenna, "A Low Cost Indoor Positioning System Using Bluetooth Low Energy," IEEE Access, vol. 8, pp. 136858-136871, 2020.
[12] Z. Munadhil, S. K. Gharghan, A. H. Mutlag, A. Al-Naji, and J. Chahl, "Neural network-based Alzheimer's patient localization for wireless sensor network in an indoor environment," IEEE Access, vol. 8, pp. 150527-150538, 2020.
[13] A. Attiya, A. Bayram, A. Safaai-Jazi, and S. Riad, "UWB applications for through-wall detection," in IEEE Antennas and Propagation Society Symposium, 2004., 2004, vol. 3: IEEE, pp. 3079-3082.
[14] D. Dardari, A. Conti, U. Ferner, A. Giorgetti, and M. Z. Win, "Ranging with ultrawide bandwidth signals in multipath environments," Proceedings of the IEEE, vol. 97, no. 2, pp. 404-426, 2009.
[15] M. Z. Win, P. C. Pinto, and L. A. Shepp, "A mathematical theory of network interference and its applications," Proceedings of the IEEE, vol. 97, no. 2, pp. 205-230, 2009.
[16] M. Z. Win, G. Chrisikos, and A. F. Molisch, "Wideband diversity in multipath channels with nonuniform power dispersion profiles," IEEE transactions on wireless communications, vol. 5, no. 5, pp. 1014-1022, 2006.
[17] A. F. Molisch, "Ultrawideband propagation channels-theory, measurement, and modeling," IEEE transactions on vehicular technology, vol. 54, no. 5, pp. 1528-1545, 2005.

TABLE 9: Summary of mean localization error of the proposed methods and previous related works

Ref./year	Wireless technology	Localization technique	Dataset	Error [m]
[7]/2017	Wi-Fi	kernel-SVM	RSSI	1.81
[8]/2017	Wi-Fi	PCA-SVM	RSS	1.37
[22]/2018	UWB	CNN combined with the WLS	CIR	0.3
[9]/2019	WiFi	CNN-CSI	CSI	0.92
[10]/2019	WiFi	LSTM	RSSI	0.75
[11]/2020	Bluetooth	Random-Forest	RSSI	0.64
[12]/2020	ZigBee	BP-ANN	RSSI	0.921
[25]/2020	UWB	DAE-BP	TDOA	0.03
[23]/2021	UWB	DLSTM	TOA	0.05
[24]/2021	UWB	DGRU	CIR	0.8
This work	**UWB**	**CNN-CSI**	**Hybrid data**	**1.53**
This work	**UWB**	**MLP**	**Received signal power**	**0.2**
This work	**UWB**	**DGRU**	**Received signal power**	**0.2**
This work	**UWB**	**DGRU**	**Received signal time**	**0.1**
This work	**UWB**	**CNN combined with the WLS**	**Hybrid data**	**0.09**
This work	**UWB**	**MLP**	**Received signal time**	**0.09**
This work	**UWB**	**MLP**	**Hybrid data**	**0.08**
This work	**UWB**	**CNN**	**Received signal power**	**0.08**
This work	**UWB**	**SVM**	**Extracted features**	**0.05**
This work	**UWB**	**CNN**	**Received signal time**	**0.04**
This work	**UWB**	**MLP**	**Extracted features**	**0.03**
This work	**UWB**	**CNN**	**Hybrid data**	**0.03**

[18] I. Güvenç, C.-C. Chong, F. Watanabe, and H. Inamura, "NLOS identification and weighted least-squares localization for UWB systems using multipath channel statistics," EURASIP Journal on Advances in Signal Processing, vol. 2008, pp. 1-14, 2007.

[19] S. Marano, W. M. Gifford, H. Wymeersch, and M. Z. Win, "NLOS identification and mitigation for localization based on UWB experimental data," IEEE Journal on selected areas in communications, vol. 28, no. 7, pp. 1026-1035, 2010.

[20] H. Wymeersch, S. Maranò, W. M. Gifford, and M. Z. Win, "A machine learning approach to ranging error mitigation for UWB localization," IEEE transactions on communications, vol. 60, no. 6, pp. 1719-1728, 2012.

[21] K. Gururaj, A. K. Rajendra, Y. Song, C. L. Law, and G. Cai, "Real-time identification of NLOS range measurements for enhanced UWB localization," in 2017 International Conference on Indoor Positioning and Indoor Navigation (IPIN), 2017: IEEE, pp. 1-7.

[22] K. Bregar and M. Mohorčič, "Improving indoor localization using convolutional neural networks on computationally restricted devices," IEEE Access, vol. 6, pp. 17429-17441, 2018.

[23] A. Poulose and D. S. Han, "Feature-Based Deep LSTM Network for Indoor Localization Using UWB Measurements," in 2021 International Conference on Artificial Intelligence in Information and Communication (ICAIIC), pp. 298-301, 2021.

[24] D. T. A. Nguyen, J. Joung, and X. Kang, "Deep Gated Recurrent Unit-Based 3D Localization for UWB Systems," IEEE Access, vol. 9, pp. 68798-68813, 2021.

[25] X. Ye and Y. Zhang, "Research on UWB positioning method based on deep learning," in 2020 5th International Conference on Mechanical, Control and Computer Engineering (ICMCCE), pp. 1505-1508, 2020.

[26] M. Ghavami, L. Michael, and R. Kohno, Ultra wideband signals and systems in communication engineering. John Wiley & Sons, 2007.

[27] A. F. Molisch et al., "IEEE 802.15. 4a channel model-final report," IEEE P802, vol. 15, no. 04, p. 0662, 2004.

[28] A. A. Saleh and R. Valenzuela, "A statistical model for indoor multipath propagation," IEEE Journal on selected areas in communications, vol. 5, no. 2, pp. 128-137, 1987.

[29] N. Ayoobi, M. Ghavami, and A. M. Rabiei, "A novel motion-model-free UWB short-range positioning method," Signal, Image and Video Processing, pp. 1-6, 2019.

[30] A. F. Molisch, "Ultra-wide-band propagation channels," Proceedings of the IEEE, vol. 97, no. 2, pp. 353-371, 2009.

[31] C.-C. Chang and C.-J. Lin, "LIBSVM: A library for support vector machines," ACM transactions on intelligent systems and technology (TIST), vol. 2, no. 3, pp. 1-27, 2011.

[32] I. Sutskever, J. Martens, G. Dahl, and G. Hinton, "On the importance of initialization and momentum in deep learning," in International conference on machine learning, 2013, pp. 1139-1147.

[33] R. Caruana, S. Lawrence, and C. L. Giles, "Overfitting in neural nets: Backpropagation, conjugate gradient, and early stopping," in Advances in neural information processing systems, 2001, pp. 402-408.

[34] R. Hongyo, Y. Egashira, and K. Yamaguchi, "Deep neural network based predistorter with relu activation for doherty power amplifiers," in 2018 Asia-Pacific Microwave Conference (APMC), 2018: IEEE, pp. 959-961.

[35] T. Dozat, "Incorporating nesterov momentum into adam," 2016.

[36] A. Krogh and J. A. Hertz, "A simple weight decay can improve generalization," in Advances in neural information processing systems, 1992, pp. 950-957.

[37] J. Tompson, R. Goroshin, A. Jain, Y. LeCun, and C. Bregler, "Efficient object localization using convolutional networks," in Proceedings of the IEEE conference on computer vision and pattern recognition, 2015, pp. 648-656.

LEYLA NOSRATI received the B.Sc. degree from the University of Bonab, Bonab, Iran, in 2017, and the M.Sc. degree in electrical engineering from the Isfahan University of Technology, Isfahan, Iran, in 2020. Her research interests include indoor localization, signal processing, machine learning, Ultra Wideband technology, and unmanned aerial vehicle (UAV) communications.

MOHAMMAD SADEGH FAZEL received the B.Sc. degree in electrical engineering (Electronics) from the Isfahan University of Technology (IUT), Isfahan, Iran, the M.Sc. degree in electrical engineering (Telecommunication Systems) University of Tehran, Tehran, Iran, and the Ph.D. degree in Wireless Communication Systems, Centre for Communication Systems Research from the University of Surrey, Guildford, Surrey, UK. In 2011, he joined the Department of Electrical and Computer Engineering at IUT as an Assistant Professor. His research interests include physical layer of wireless communication systems, including massive MIMO systems, beamforming and NOMA, signal processing, and telecommunication in general.

MOHAMMAD GHAVAMI is currently a Professor of telecommunications with the London South Bank University. Prior to this appointment, he was with King's College London, from 2002 to 2010, and with the Sony Computer Science Laboratories, Tokyo, from 2000 to 2002. He has authored the books, namely the Ultra Wideband Signals and Systems, and the Adaptive Antenna Systems, and has published over 180 technical papers mainly related to UWB and its medical applications. He holds three US and one European patents. He won the esteemed European Information Society Technologies Prize, in 2005, and two invention awards from Sony. He has been the Guest Editor of the IET Proceedings Communications, the Special Issue on Ultra Wideband Systems, and the Associate Editor of the Special Issue of the IEICE Journal on UWB Communications.